Scientific paper

Simplified Inverse Method for Determining the Tensile Properties of Strain Hardening Cementitious Composites (SHCC)

Shunzhi Qian[1] and Victor C. Li[2]

Received 19 February 2008, accepted 28 April 2008

Abstract

As an emerging advanced construction material, strain hardening cementitious composite (SHCC) has seen increasing field applications in recent years. Reliable data on tensile properties, including tensile strength and tensile strain capacity, are needed for structural design and for quality control. However, existing uniaxial tensile tests are relatively complicated and sometime difficult to implement, particularly for quality control purpose in the field. A simple inverse method based on beam bending test was presented by the authors (Qian and Li, 2007) for indirect determination of tensile strain capacity, aimed at quality control of SHCC in field applications. This paper extends this method to also determining the tensile strength based on beam bending test data. This proposed method (UM method) has been validated with uniaxial tensile test results with reasonable agreement. In addition, this proposed method is also compared with the Japan Concrete Institute (JCI) method. Comparable accuracy is found, yet the present method is characterized by much simpler experiment setup requirement and data interpretation procedure. Therefore, it is expected that this proposed method can greatly simplify the quality control of SHCCs both in execution and interpretation phases, contributing to the wider acceptance of this type of new material in field applications.

1. Introduction

In the past decade, great strides have been made in developing strain hardening cementitious composite (SHCC), characterized by its unique macroscopic pseudo strain hardening behavior after first cracking under uniaxial tension. SHCCs, also referred to as high performance fiber reinforced cementitious composites (HPFRCCs, Naaman and Reinhardt 1996), develop multiple cracks under tensile load in contrast to single crack and tension softening behavior of concrete and conventional fiber reinforced concrete. Multiple cracking provides a means of energy dissipation at the material level and prevent catastrophic fracture at the structural level, thus contributing to structural safety. Meanwhile, material tensile strain hardening (ductility) has been gradually recognized as having a close connection with structural durability (Li 2004) by suppressing localized cracks with large width. Many deterioration and premature failure of infrastructure can be traced back to the brittle nature of concrete. Therefore, SHCCs are considered a promising material solution to the global infrastructure deterioration problem and its tensile behavior is of major interest.

[1]Formerly graduate student, Department of Civil and Environmental Engineering, University of Michigan, Ann Arbor; Now postdoctoral researcher, Microlab, Faculty of Civil Engineering and Geosciences, Delft University of Technology, the Netherlands.
[2]Professor, Department of Civil and Environmental Engineering, University of Michigan, U S A.
*E-mail:*vcli@umich.edu

While most characterization of the tensile behavior of SHCCs was carried out using uniaxial tensile test (UTT) in academia, this method is generally considered to be complicated, time-consuming and require advanced equipment and delicate experimental skills. Therefore, it is not suitable for onsite quality control purpose (Stang and Li 2004, Ostergaard *et al* 2005, Kanakubo 2006).

As a simpler alternative to the UTT, four point bending test (FPBT) was proposed by Stang and Li (2004) for quality control on construction sites, provided that an appropriate interpretation (inverse) procedure for the test result is available. This type of test is much simpler and puts much less demand on equipment and experimental skills compared to UTT, and extensive experience has been accumulated in the user community. The ultimate goal of this test is to use the moment-curvature or moment-deflection curves so determined to invert for the uniaxial tensile properties. It should be noted, however, that the bending test is not meant to determine whether the material has tensile strain-hardening behavior or tension-softening behavior, but rather to constrain the material tensile properties, e.g. the tensile strain capacity or tensile strength, as part of the quality control process in the field, for a material mix designed to exhibit strain-hardening. The inverse procedure is the key to the success of FPBT to achieve the intended purpose, and it must be sufficiently accurate yet simple enough for field practice.

Inverse analyses for FPBT have recently been attempted by researchers at Technical University of Denmark (DTU), Japan Concrete Institute (JCI) and University of Michigan (UM) (Ostergaard *et al* 2005; Kanakubo 2006; Qian and Li 2007) with certain success. Both the JCI and UM methods are based on a simplified

elastic-plastic tensile model and can generally predict tensile properties from the FPBT results via a sectional analysis similar to that developed by Maalej and Li (1994). On the other hand, hinge model, including both tensile strain hardening and tension softening effect, was employed in the DTU inverse method along with least square method to invert for tensile material properties from their bending response. The model can predict experimental load – deflection curve fairly well and tensile properties derived based on this method agree well with that from FEM analysis, yet no direct comparison with UTT results has been made so far.

The UM method may be more appealing to the user community compared with the JCI method due to improvement in terms of experimental execution (no need for LVDTs) and data interpretation procedure (simple linear transformation instead of relatively complicated procedure) yet with similar accuracy (Qian and Li 2007). Nevertheless, unlike the JCI method, the existing UM method can only predict tensile strain capacity, which sometimes can limit its usefulness for quality control of SHCCs. In large scale field application of SHCCs, tensile strength has also been commonly monitored besides tensile strain capacity due to its importance in the structural application (Kanda *et al* 2006; Lepech 2006). Therefore, the UM method has to be further developed to be able to predict the tensile strength in order to make it an efficient and comprehensive quality control method for SHCCs materials.

In this paper, the UM method will be extended to incorporate tensile strength prediction, in addition to its existing prediction capability for tensile ductility. In the following sections, the overall research framework for the extended UM method will be presented first, followed by parametric study to obtain the master curves for inverse analysis. Thereafter, the experimental program consisting of both FPBT and complementary UTT will be briefly reviewed. The results from FPBT will then be converted to tensile strength and validated with independent UTT test results. Finally, the extended UM method will be compared with JCI inverse method, followed by overall conclusions.

2. Overall research framework

The overall research framework is revealed in **Fig. 1**, consisting of detailed procedure for development and execution of inverse method (top frame (a)) and validation and verification procedure (bottom frame (b)). As shown in the top frame (a), MOR and corresponding deflection capacity can be obtained from FPBT. By conducting parametric studies based on a flexural behavior model of SHCCs, a master curve can be constructed in terms of MOR/effective tensile strength with respect to tensile strain capacity. Based on predicted tensile strain capacity from authors' previous work (Qian and Li 2007) and master curve from parametric study, effective tensile strength of SHCCs can be derived. Based on the research framework, a detailed inverse procedure for the extended UM method is revealed in **Fig. 2**.

Additionally, companion UTT tests using specimens cast from the same batch of material is used to validate and/or verify the UM method in terms of the accuracy of the derived tensile strength, which is shown in the bottom frame (b). It is conceived that a large number of FPBT will be conducted at construction sites on a daily basis to ensure the quality of the SHCC material. The extra step of verification (Frame (b)) will not be necessary once the method is standardized and utilized in practice, except for a very limited number of UTT specimens to be cast onsite and tested at advanced research laboratory to confirm that this material is truly a strain hardening type during the trial mixing stage.

3. Parametric study and master curves

3.1 Flexural behavior model

The flexural behavior model used in this investigation is based on the work of Maalej and Li (1994). Compared with other models, the major distinction of this model is that the contribution of tensile strain hardening property of SHCCs was included. The actual SHCC considered

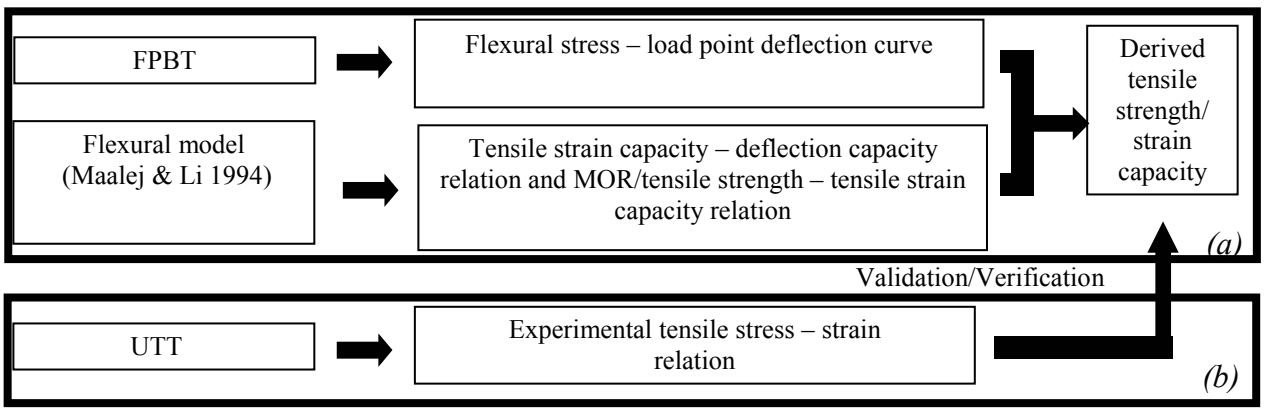

Fig. 1 Overall research framework for extended UM method.

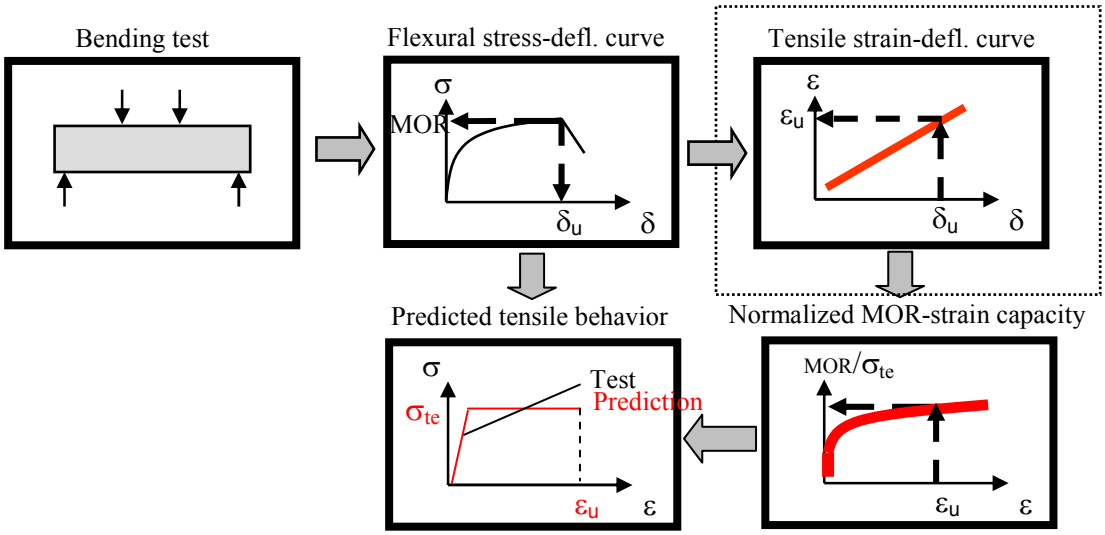

Fig. 2 Sketch of inverse procedure of extended UM method (Tensile strain-deflection curve shown in dash-line box is the master curve developed in Qian and Li (2007); δ_u: is the deflection capacity corresponding to the MOR in flexural stress-deflection curve; ε_u:is the predicted tensile strain capacity inversed from deflection capacity; σ_{te}: is the predicted effective tensile strength).

in the model is Polyethylene ECC (PE-ECC) material, with uniaxial tensile and compression stress-strain curves schematically shown as dashed line in **Fig. 3 (a)** and **(b)**. To simplify the analysis, the stress-strain behavior of the ECC was assumed as bilinear curves in both tension and compressive, shown as the solid lines in **Fig. 3 (a)** and **(b)**. Based on a linear strain profile and equilibrium of forces and moment in the beam section, the relation between flexural stress and tensile strain at the extreme tension fiber (Simplified as critical tensile strain hereafter) can be determined as a function of basic material properties. Due to the linear relation between critical tensile strain and deflection, the flexural stress and deflection relation can then be established. Overall, the model predicts experimentally measured flexural response quite well. For more detail, the readers are referred to Maalej and Li (1994).

As an illustration of capability of the model, **Fig. 4** shows the variation of the modulus of rupture over first cracking strength (MOR/σ_{tc}) ratio as a function of the ultimate tensile strain (ε_{tu}) for the 2% polyethylene ECC (assuming that ε_{tu} can be varied without changing the other properties of the composite) (Maalej and Li 1994). This figure indicates that the MOR/σ_{tc} ratio increases as a function of ε_{tu}. The rate of increase is initially high, and as ε_{tu} becomes larger than 0.01, the rate of increase becomes very small. The model indicates that the initial high slope of the (MOR/σ_{tc})-ε_{tu} curve is associated with a significant increase in the size of the microcracking zone as the ultimate tensile strain increases. When ε_{tu} becomes large, the size of the microcracking zone reaches about 90% of the beam depth and does not significantly change as ε_{tu} continues to in-

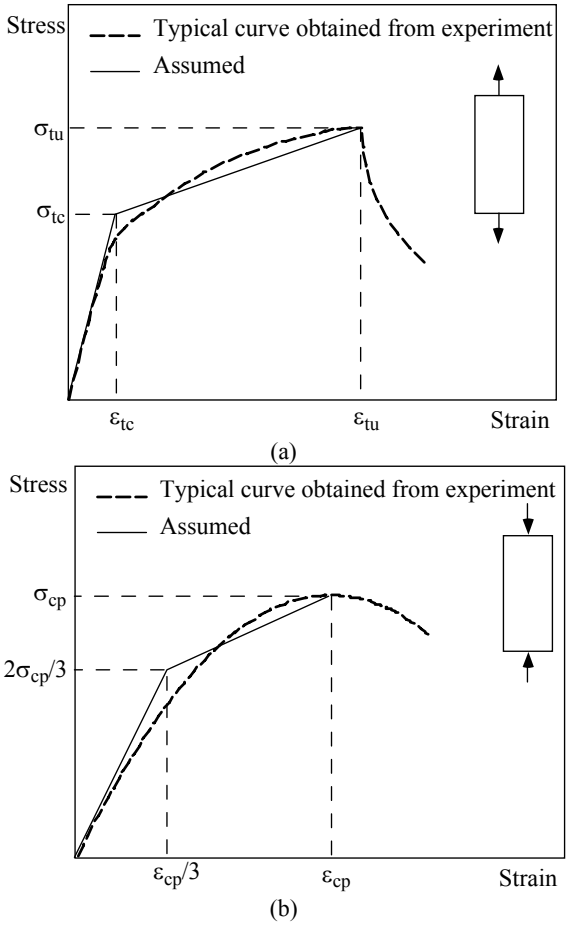

Fig. 3 Stress-strain relation of PEECC in (a) uniaxial tension and (b) uniaxial compression (Adopted from Maalej and Li 1994).

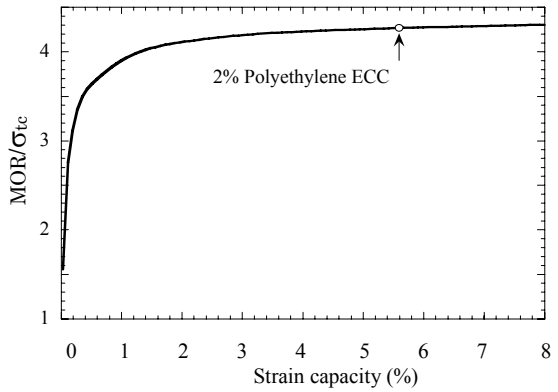

Fig. 4 Variation of the MOR/σ_{tc} Ratio as a function of tensile strain capacity (ε_{tu}).

crease. This suggests that the MOR of the polyethylene ECC would not significantly change as a result of an increase in the ultimate tensile strain of the material beyond about 1%. On the other hand, the MOR of the polyethylene ECC can be increased by increasing the tensile first cracking strength and/or the ultimate tensile strength.

While the above (MOR/σ_{tc})-ε_{tu} relation is derived based on only one particular SHCC (PE-ECC) by varying its tensile strain capacity and resulting in different MOR, it does suggest that such a relation, if holds true for a wide range of material tensile and compressive properties, will provide a basis for inverse analysis of the tensile strength from MOR. This will be investigated in the following parametric studies and a master curve to correlate the ratio of MOR to tensile strength with ε_{tu} will be established. To simplify the inverse process and minimize the unknowns, however, it is advisable to assume that the hardening modulus of SHCCs in tension is zero, i.e, the first cracking strength is equal to the ultimate tensile strength.

3.2 Construction of master curves

A parametric study was conducted to investigate the influence of material uniaxial tensile and compressive properties (parametric values) on the flexural response of SHCCs based on the aforementioned flexural model. To simplify the inverse process, the first cracking strength is assumed to be equal to the ultimate tensile strength and will be labeled as the effective tensile strength hereafter. The correlation between the normalized MOR (by effective tensile strength) and the tensile strain capacity was established. All tensile and compressive properties were varied within a wide range of parametric values (**Table 1**), covering the normal range of test results of SHCC specimens at UM and JCI (Kanakubo 2006). It is expected that the master curves based on this wide range of parametric study can be directly utilized for quality control purpose in field.

The overall results from the parametric study indeed show a fairly good correlation between the normalized MOR and the tensile strain capacity, as revealed in **Fig. 5(a)**. Totally 20 cases were investigated in the parametric study, with the range of material parameters shown in **Table 1**. All curves lie in a relatively narrow band regardless of actual material properties, which suggests that the normalized MOR is most sensitive to the tensile strain capacity, at least when the tensile strain is less than 1%. Normalized MOR shows a plateau when the tensile strain exceeds 1%, which suggests that it is almost independent of tensile strain capacity. For ease of quality control on site, master curve was constructed with two lines to cover all parametric case studies, as shown in **Fig. 5 (b)**.

It is well known that for an elastic-perfectly plastic material like metal, the normalized MOR (MOR/σ_{tc}) is equal to 3, in which case σ_{tc} is the yield strength. For an elastic-ideally brittle material like glass, the normalized MOR is equal to 1. **Figure 5** shows that for SHCC material, this same ratio is bracketed between 1 and 3 depending on the tensile strain capacity. Note that for SHCC, the compression block does not follow the elastic-perfectly plastic behavior (**Figs. 3(b)** and **6**). **Figure 4** shows that for SHCC material with tensile strain-hardening, the normalized MOR can reach above 3.

Additionally, another master curve correlating the normalized MOR with the tensile strain capacity was constructed by parametric study based on the JCI standard beam specimen in order to compare the proposed UM method with the JCI method. The range of material parametric values is the same as the aforementioned parametric study in **Table 1**. The dimension of the specimens used in this parametric study is

Table 1 Range of material parameters used in parametric studies to construct the normalized MOR - tensile strain capacity relation.

	Tensile properties			Compressive properties	
Material parameters	Effective tensile strength (MPa)	Tensile strain capacity (%)	Modulus of elasticity (GPa)	Compressive strength (MPa)	Compressive strain capacity (%)
Range	2.5~16.0	0~5	12~53	31~200	0.5~1*

Note: Parameters are in the normal range of test results of SHCC specimens at UM and JCI; Tensile and compressive modulus of elasticity are assumed to be equal; Beam dimensions are 51x76x356mm and 100x100x400mm with span length of 305mm and 300mm for UM and JCI specimens, respectively; *: Estimated range.

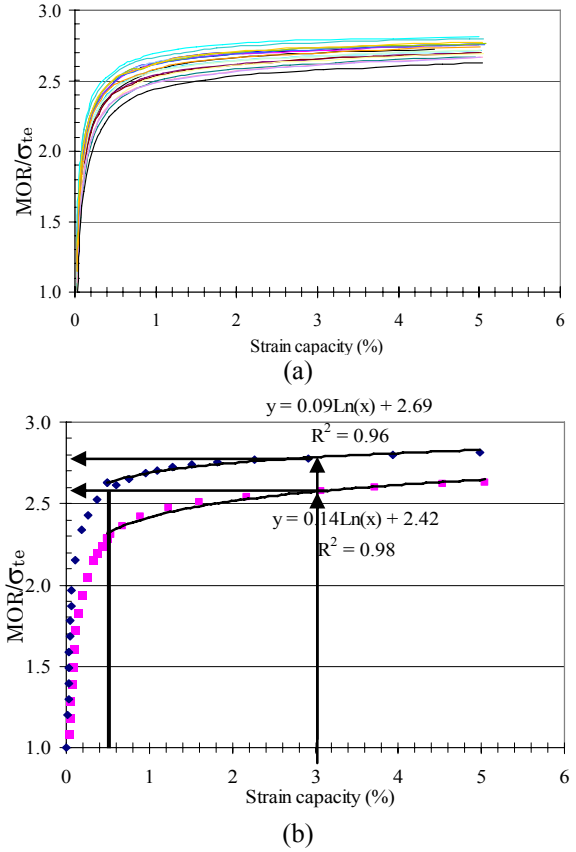

Fig. 5 Relation of MOR/σ_{te} with tensile strain capacity for (a) all cases with UM and JCI data (smoothed lines from actual data points) and (b) two extreme cases with up and lower boundaries (It is not recommended to use this master curve to invert for σ_{te} when the strain capacity is less than 0.5%; y and x means MOR/σ_{te} and strain capacity, respectively).

100x100x400mm, with a span length of 300mm (JCI-S-003-2007).

As expected, this set of master curve coincides with the one shown in **Fig. 5**, especially in terms of upper bound and lower bound. This can be understood from the fact that the normalized MOR is a dimensionless number, which should be independent of geometry (beam height) of specimen. It should be noted however that the master curve relating deflection capacity to tensile strain capacity is dependent on the geometry of the specimen (Qian and Li 2007). When two master curves are expected to be used together for quality control, a standard size of specimen should be specified.

3.3 Discussion on the unique behavior of master curves

The master curve reveals a plateau with a relatively narrow band width when tensile strain capacity exceeds 1%. In the following, discussions will be presented to provide some understanding of this unique phenomenon.

As shown in **Fig. 6**, a simple model of sectional

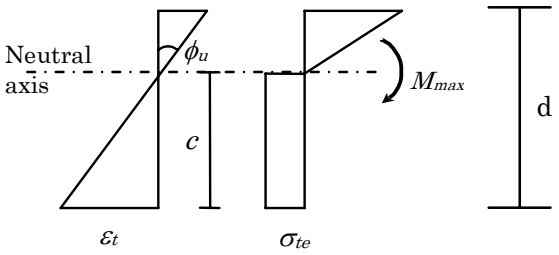

Fig. 6 Assumption of strain and stress distribution along beam section.

analysis similar to Kanakubo (2006) was adopted to facilitate the easy derivation of the relation of normalized MOR with tensile strain capacity. When tensile strain capacity is sufficiently large, e.g. 1%, the result from this simple model should yield comparable result to that from more complicated model such as Maalaj and Li model (1994), which was used in the parametric study to obtain the master curve.

From both force equilibrium and moment equilibrium, following two equations can be derived:

$$\frac{E \cdot b \cdot \phi_u}{2} \cdot (d-c)^2 = \sigma_{te} \cdot b \cdot c \tag{1}$$

$$M_{max} = \frac{E \cdot b \cdot \phi_u}{3} \cdot (d-c)^3 + \frac{\sigma_{te} \cdot b}{2} \cdot c^2 \tag{2}$$

where E is the static modulus of elasticity (N/mm^2); b is the width of specimen (mm); ϕ_u is the curvature capacity (1/mm); d is the depth of the specimen (mm); c is the distance from extreme tension fiber to the neutral axis (mm); σ_{te} is the predicted effective tensile strength (MPa); M_{max} is the maximum moment $(N \cdot mm)$.

The above equations can be simplified to obtain the expression for effective tensile strength and MOR as follows:

$$\sigma_{te} = \frac{E \cdot \phi_u}{2c} \cdot (d-c)^2 \tag{3}$$

$$MOR = \frac{6M_{max}}{bd^2} = 2E \cdot d \cdot \phi_u \cdot (1-\frac{c}{d})^3 + 3\sigma_{te} \cdot (\frac{c}{d})^2 \tag{4}$$

The ratio of MOR over effective tensile strength can then be derived as a function of c_0 or c/d:

$$\frac{MOR}{\sigma_{te}} = 4(\frac{c}{d}) - (\frac{c}{d})^2 = 4c_0 - c_0^2 \tag{5}$$

According to Qian and Li (2007), c_0 shows a plateau value of around 0.9 once ε_{tu} exceeds 1%, as can be seen in **Fig. 7**. The corresponding normalized MOR is about 2.8, which agrees reasonably well with the master curve shown in **Fig. 5**. Furthermore, it is observed that these c_0 values near plateau are very close for cases with drasti-

cally different material properties. This explains the narrow band width of the master curve. It should be noted, however, that the above equation (5) should not be used for cases when ε_{tu} is well below 1%, e.g. when c_0 equals to 0.5 (corresponding ε_{tu} of 0%) due to the great simplification of stress distribution mentioned previously.

3.4 Use method of master curves

Based on the master curves obtained from parametric study, the MOR from simple beam bending test can be easily converted to effective tensile strength, with detailed procedure schematically shown in **Fig. 5b** and explained below. Assuming a tensile strain capacity of 3% already being inverted from deflection capacity, the corresponding value of MOR/σ_{te} can then be found from the master curve, including both upper and lower bound values (2.8 and 2.58 respectively). Assuming an MOR of 12 MPa obtained from experimental bending test, the effective tensile strength will then be 4.29 MPa and 4.65 MPa. In order to be on the conservative side for quality control purpose, the upper boundary of the master curve may be used, which will give a lower value of effective tensile strength. The calculation of standard deviation of the effective tensile strength can then use the same upper bound value given the standard deviation of MOR is known. The master curve is not recommended for use for tensile strain capacity less than 0.5% due to the steep slope of the master curve at the initial stage.

A set of equations has been developed by curve fitting (**Fig. 5b**) to simplify the conversion procedure, as shown below, where Equations (6) and (7) can be used to calculate the effective tensile strength, including both lower limit σ_{te}^{1} and upper limit σ_{te}^{2}, respectively.

$$\sigma_{te}^{1} = \frac{MOR}{0.09Ln(\varepsilon_{tu}) + 2.69} \tag{6}$$

$$\sigma_{te}^{2} = \frac{MOR}{0.14Ln(\varepsilon_{tu}) + 2.42} \tag{7}$$

where ε_{tu} is the tensile strain capacity (%), Ln is natural logarithm and R^2 is 0.96 and 0.98 for Equations (6) and (7), respectively.

As mentioned previously, the master curve can only be applied for use for tensile strain capacity larger than 0.5% due to the steep slope of the master curve at the initial stage. Similarly, the above equations can only be utilized for derivation of effective tensile strength when the tensile strain capacity exceeds 0.5%.

4. Experimental setup and results

The mix proportion of SHCC materials investigated in this study is shown in **Table 2**, including PVA-ECC 1, 2 and 3. These SHCC materials feature high amount of fly ash in the mix proportion, with fly ash to cement ratios of 1.2, 2.0, and 2.8, respectively. Additionally, SHCCs with PVA, PE and hybrid fibers (PE and steel fibers, simplified as HB) and steel fiber (simplified as SF) from Kanakubo (2006) are also listed in **Table 2**, which will be used for comparison between the UM method and the JCI method.

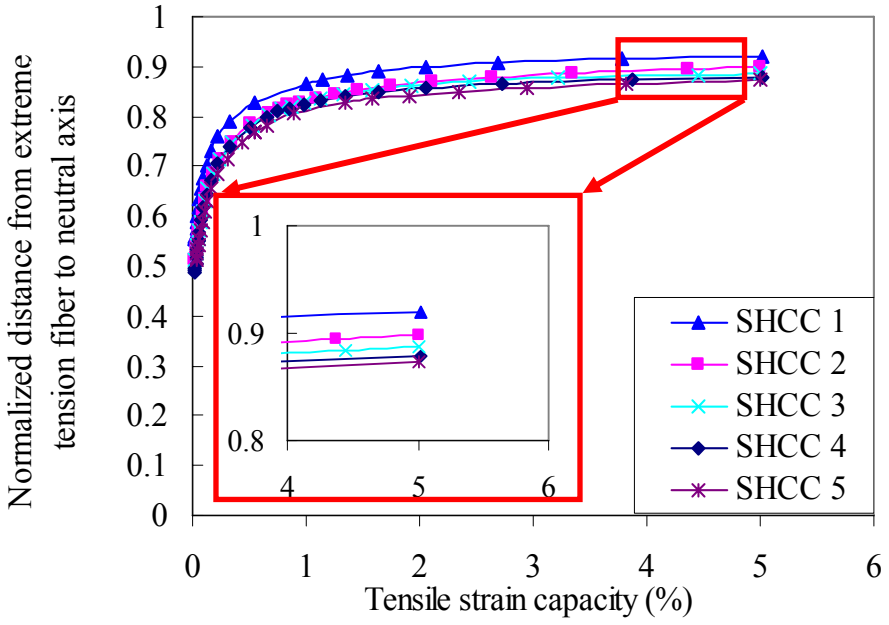

Fig. 7 Normalized distance from extreme tension fiber to neutral axis (distance normalized by the beam height) – tensile strain capacity (c_0– ε_{tu}) relation for SHCCs.

A Hobart mixer was used in this investigation, with a full capacity of 12 liters. All beam, uniaxial tensile and compressive specimens were cast from the same batch. The beam and uniaxial tensile specimens were cast horizontally and compressive cylinder specimens were cast vertically. At least 3 specimens were prepared for each test. After demolding, all specimens were cured in a sealed container with about 99% humidity under room temperature for 28 days before testing. Four point bending test was conducted with a MTS 810 machine. The

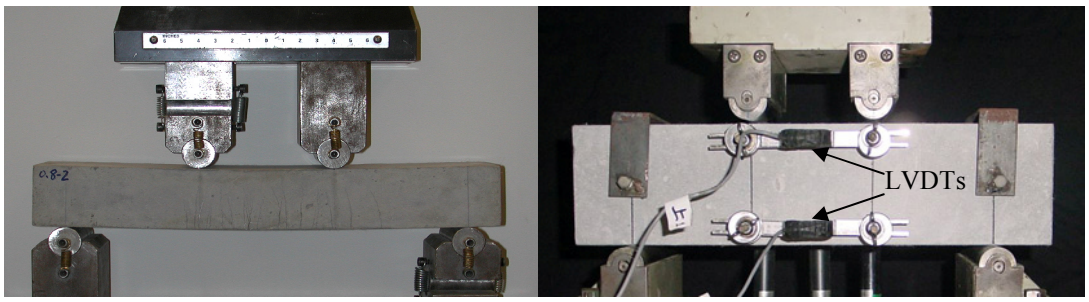

(a) (b)

Fig. 8 Comparison of test setup for the (a) UM method and (b) JCI method (Beam deflection at the loading points was obtained from machine displacement directly in UM method).

Table 2 Mix proportion for different SHCCs.

	Cement	Sand	Fly ash	Water/cementitious materials	Superplasticizer	Fiber
PVA-ECC 1	1	0.8	1.2	0.27	0.013	0.02
PVA-ECC 2	1	1.1	2	0.26	0.014	0.02
PVA-ECC 3	1	1.4	2.8	0.26	0.016	0.02
PVA-SHCC*	-	-	-	0.46	-	0.019
PE-SHCC*	-	-	-	0.30	-	0.015
HB-SHCC*	-	-	-	0.45	-	0.01/0.01**
SF-SHCC*	-	-	-	0.22	-	0.02

Note: *:Data from JCI round robin test (Kanakubo, 2006); **:hybrid fibers SHCC with 1% PE and 1% steel fiber

Table 3 Tensile properties from 2D UTT test and compressive strength for PVA-ECC 1, 2 and 3 and other SHCCs.

	First cracking strength (MPa)	Ultimate tensile strength (MPa)	Tensile strain capacity (%)	Compressive strength (MPa)
PVA-ECC 1	4.6±0.3	5.3±0.6	2.1±1.1	54.6±6.5
PVA-ECC 2	3.9±0.5	4.6±0.2	3.5±0.3	46.0±3.8
PVA-ECC 3	4.0±0.2	4.9±0.1	3.7±0.4	37.5±1.7
PVA-SHCC*	3.7±0.8	5.0±0.5	2.7±0.7	31.3±0.8
PE-SHCC*	3.0±0.5	4.9±0.5	1.3±0.3	67.3±1.8
HB-SHCC*	2.3±0.2	4.4±0.6	0.7±0.3	43.6±2.7
SF-SHCC*	13.7±0.9	15.3±1.0	0.5±0.3	198.0±3.7

Note: *:Experimental data from JCI round robin test (Kanakubo, 2006).

Table 4 Material tensile properties from 3D UTT test and bending properties for different SHCCs (Kanakubo 2006).

	First cracking strength (MPa)	Ultimate tensile strength (MPa)	MOR (MPa)	Curvature (μ/mm)
PVA-SHCC	3.2±0.8	3.4±0.4	9.2±0.9	349.2±96.3
PE-SHCC	5.1±0.6	5.6±0.3	13.3*	269.6*
HB-SHCC	2.7±0.6	2.8±0.8	9.2±3.2	213.4±147.6
SF-SHCC	9.4*	12.4*	27.1±0.7	80.0±40.0

Note: *:only one test data point was obtained.

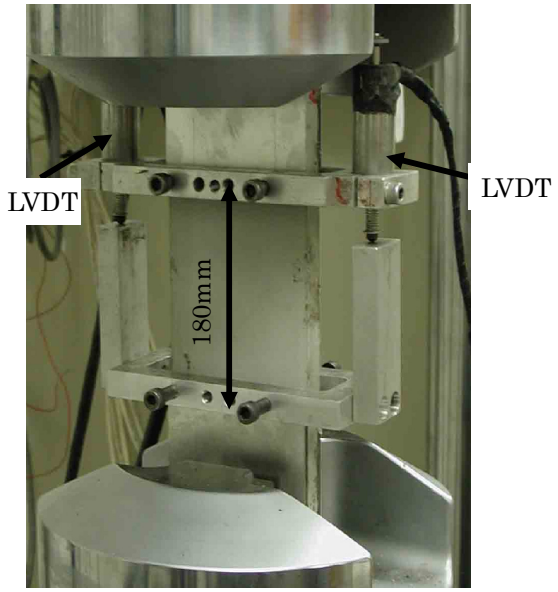

Fig. 9 Setup for uniaxial tensile test.

test setup is shown in **Fig. 8 (a)** in comparison with the JCI method (**Fig. 8 (b)**). As shown in **Fig. 9**, uniaxial tensile test (UTT) with "fix-fix" end condition was also carried out to directly verify the derived effective tensile strength from four point bending test. For more details on the experiments, the readers are referred to Qian and Li (2007).

Two types of uniaxial tensile test results along with bending test results (Kanakubo 2006) are also included as independent data for comparison between the UM method and the JCI method, including both 2D and 3D fiber distribution specimens. The 2D uniaxial tensile test involves plate type specimen with a 30 x 13 mm cross section (Kanda and Li 1999). Due to its small cross section compared with fiber length of 12 mm, it can be regarded as having a two dimensional fiber orientation, similar to the UM UTT test. The other type has a 70 mm circular section, which is shaped using a cylinder mold (Furuta *et al*. 2003). A "pin-fix" end condition was selected for both tensile tests.

The material tensile, compressive properties and bending properties for different SHCCs can be found in **Tables 3** and **4**. Furthermore, uniaxial tensile stress-strain curves and bending stress-deflection curves from PVA-ECC 1, 2 and 3 are shown in **Figs. 10** and **11**. As revealed from **Fig. 11**, PVA-ECC 1-3 show typical deflection hardening behavior under FPBT. The defection capacity and corresponding MOR obtained from these curves can then be used to invert the tensile strain capacity and effective tensile strength, as shown in **Figs. 2** and **5**.

5. Validation and verification of the proposed method

To validate the proposed inverse method, the MOR obtained from FPBT is converted to effective tensile strength using Equations (6) and (7) and then compared with first cracking strength and/or tensile strength obtained directly from uniaxial tensile test for PVA-ECC 1-3. As revealed in **Table 5** and **Fig. 12**, the effective tensile strength (both lower and upper limits) derived from FPBT seems to match the first cracking strength with reasonable accuracy, with less than 10% difference. This agreement demonstrates the validity of the proposed inverse method. Furthermore, the lower limit prediction may be used in order to be conservative for quality control purpose.

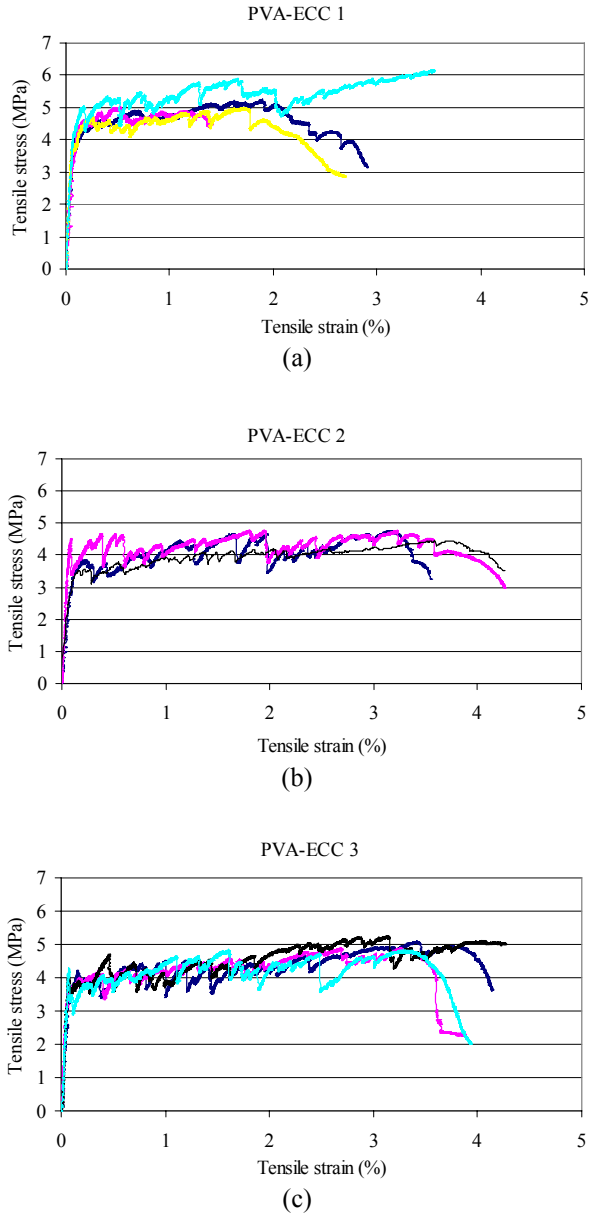

Fig. 10 Uniaxial tensile stress strain relation for (a) PVA-ECC 1,(b) PVA-ECC 2 and (c) PVA-ECC 3.

To further verify the proposed UM method, comparison between the UM method and the JCI method was conducted based on JCI round robin test data (Kanakubo 2006). As mentioned previously, the bending test results from the JCI round robin test are presented in the form of moment-curvature relation. Within the JCI method, the effective tensile strength is obtained by solving the following equations (JCI-S-003-2007):

$$f_{t,b} = \frac{E \cdot \phi_u \cdot D \cdot x_{nl}^2}{2(1 - x_{nl})} \tag{8}$$

$$x_{nl} = -1 + 2\cos\frac{\theta}{3} \tag{9}$$

$$\theta = \arccos(-1 + 6m^*) \tag{10}$$

$$m^* = \frac{M_{\max}}{E \cdot \phi_u \cdot B \cdot D^3} \tag{11}$$

where $f_{t,b}$ is the predicted effective tensile strength (MPa); E is the static modulus of elasticity (N/mm^2); ϕ_u is the curvature capacity (1/mm), which can be calculated from two LVDTs measurements (**Fig. 8 (b)**); D is depth of the test specimen (=100 mm); x_{nl} is the ratio of the distance from compressive edge (extreme compression fiber) to neutral axis over depth of test specimen, which needs to be solved from Equations (9-11); $M_{\max}$ is maximum moment $(N \cdot mm)$; B is the width of test specimen (100 mm). For more details, readers are referred to the Appendix to JCI-S-003-2007.

As shown in **Table 6** and **Fig. 13**, predictions based on both the UM method and the JCI method reveal comparable results with those from uniaxial tensile tests of 3D specimens. This is consistent with the expectation that the fiber orientation in the flexural beam geometry is probably closer to 3-D. Furthermore, the tensile test results from 2D specimens generally shows higher tensile strength compared with that from 3D specimens as expected. In particular, the tensile strength of SF-SHCC in 2D specimens may be artificially boosted by its long steel fiber (15mm) mixed within very small cross-section (13mmx30mm). Tensile strength of PE-SHCC is lower in 2D compared with that in 3D may be due to different casting direction and/or done by different groups with different fresh rheology (Kanakubo 2006). The overall consistency between the UM method and the JCI method and verification by independent JCI round robin test data further demonstrate the validity of the proposed UM method.

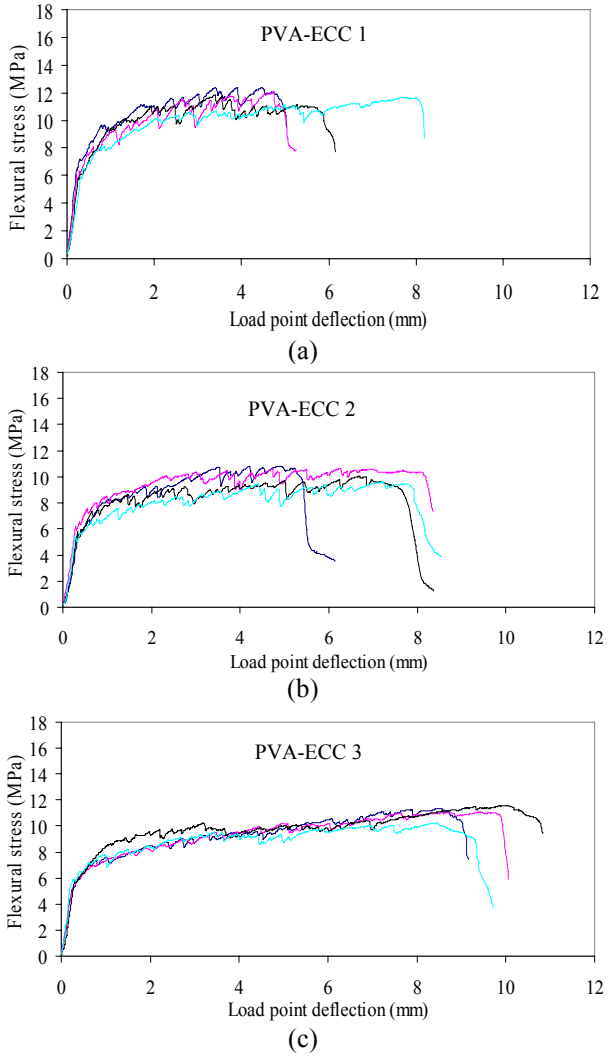

Fig. 11 Experimental flexural stress – load point deflection relation for (a) PVA-ECC 1 (b) PVA-ECC 2 and (c) PVA-ECC 3.

Table 5 Comparison between effective tensile strength predicted from FPBT and first cracking strength/tensile strength from 2D UTT test.

	First cracking strength (MPa)	Ultimate tensile strength (MPa)	Effective tensile strength (lower limit) (MPa)	Effective tensile strength (upper limit) (MPa)
PVA-ECC 1	4.6±0.3	5.3±0.6	4.3±0.1 (-7%)	4.7±0.1 (2%)
PVA-ECC 2	3.9±0.5	4.6±0.2	3.6±0.2 (-7%)	4.0±0.2 (2%)
PVA-ECC 3	4.0±0.2	4.9±0.1	3.9±0.2 (-2%)	4.2±0.2 (5%)

Note: The number in parenthesis is the difference between the predictions and first cracking strength from uniaxial tensile test (only 2D UTT is available for PVA-ECC 1-3).

The advantage of the UM method over the JCI method lies in its simplicity, both in the experimental and data interpretation phases. In the experimental phase, the UM method requires only machine displacement to be measured. This is not the case for the JCI method, where complicated setup such as LVDTs is needed to measure curvature, as revealed in **Fig. 8 (a)** and **(b)**. In the data interpretation phase, the UM method only needs a simple master curve or equation to convert MOR directly into effective tensile strength, while the JCI method requires relatively complicated procedures to obtain effective tensile strength. Considering the large amount of specimens needed to be tested during construction, the UM method seems to be more suitable for quality control purpose due to its simplicity, efficiency and reasonable accuracy.

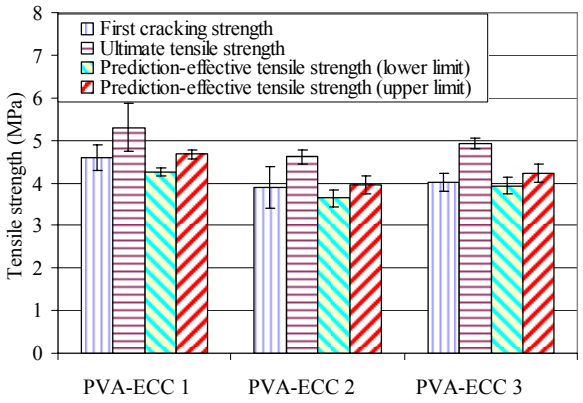

Fig. 12 Comparison of UTT results and predicted effective tensile strength based on extended UM method for PVA-ECC 1, 2 and 3.

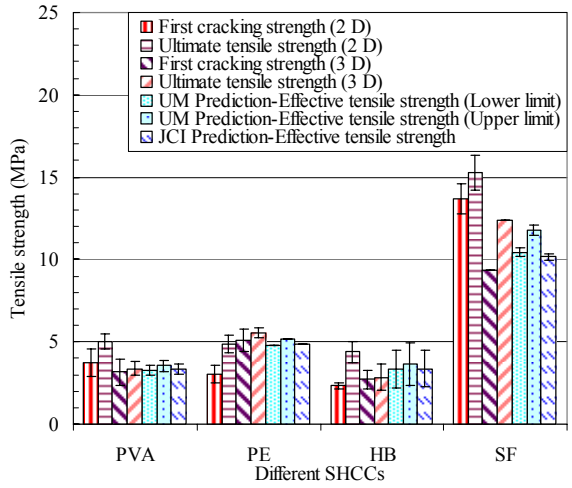

Fig. 13 Comparison of 2D and 3D UTT results and predicted effective tensile strength based on extended UM and JCI method for different SHCCs.

6. Conclusions

To facilitate the quality control of the strain hardening cementitious composites on site, a simplified inverse method is proposed to convert the MOR from simple beam bending test to effective tensile strength through simple transformation. The simple transformation (in the form of master curves) is derived from parametric study with a wide range of parametric values of material tensile and compressive properties based on a theoretical model. This proposed method has been experimentally validated with uniaxial tensile test results. In addition, this proposed method compares favorably with the JCI method in accuracy, but without the associated complexity.

The following specific conclusions can be drawn from this study:

(1) A simple inverse method has been successfully developed to derive effective tensile strength of SHCC from MOR of beam bending test by using a master curve. This method is expected to greatly ease the on-site quality control for SHCC in terms of much simpler experiment setup requirement (compared with both UTT and the JCI inverse method) and data interpretation procedure (compared with the JCI method), yet with reasonable accuracy (generally within 11% if the lower limit prediction is used for conservativeness) ;

(2) The master curve features relatively simple transformation with a narrow band width. The master

Table 6 Comparison between 3D uniaxial tensile test results with predictions based on the UM and JCI methods for different SHCCs.

	First cracking strength (MPa)	Ultimate tensile strength (MPa)	Effective tensile strength (lower limit) (MPa)	Effective tensile strength (upper limit) (MPa)	JCI predicted tensile strength (MPa)
PVA-SHCC	3.2±0.8	3.4±0.4	3.3±0.3 (4%)	3.6±0.3 (12%)	3.3±0.3 (4%)
PE-SHCC	5.1±0.6	5.6±0.3	4.8* (-6%)	5.2*(2%)	4.8* (-6%)
HB-SHCC	2.7±0.6	2.8±0.8	3.3±1.2 (23%)	3.7±1.3 (35%)	3.4±1.1 (25%)
SF-SHCC	9.4*	12.4*	10.4±0.3 (11%)	11.8±0.3 (25%)	10.2±0.2 (8%)

Note: 3D UTT test results for all four SHCCs are from Kanakubo (2006); *: Only one specimen were reported; The number in parenthesis is the difference between the predictions and first cracking strength from 3D uniaxial tensile test.

curve decouples the dependence of effective tensile strength on the curvature capacity in contrast with the JCI method where effective tensile strength is dependent on both curvature capacity and moment capacity. Therefore, this method allows relatively simple equations (Equation (6) and (7)) to be used for easy data interpretation;

(3) A plateau value of around 2.7-2.8 is observed for master curve when the strain capacity exceeds 1%. It has been shown that this plateau value is closely related to the fact that the neutral axis of the SHCCs under bending rapidly approaches the extreme compression fiber and quickly stabilizes (the plateau distance from extreme tension fiber to neutral axis is about 90% of the beam depth); Once the strain capacity exceeds 1%, the effective tensile strength is almost fully dependent on MOR only.

(4) The master curve itself is not dependent on the geometry of the specimen, in contrast to the previous master curve relating the tensile strain capacity with deflection capacity (Qian and Li, 2007). When these two sets of master curves are used together to determine both the tensile strain capacity and the effective tensile strength, however, a standard geometry of specimen must be specified.

It should be noted that the following assumptions are made when the proposed UM method is used: (a) The tested material is truly a strain hardening type; (b) The major target for quality control for this material is tensile strength and tensile ductility; and (c) For this method to be most effective, a standardized beam with fixed geometric dimensions should be agreed upon by the user community.

Acknowledgements

The authors thank the Michigan Department of Transportation, and the National Science Foundation for funding portions of this research (CMS-0223971, CMS-0329416).

References

Furuta, M., Kanakubo, T., Kanda, T. and Nagai, S. (2003). "Evaluation of uni-axial tensile model for high performance fiber reinforced cementitious composites." *Journal of Structural and Construction Engineering (Transactions of AIJ)*, 568, 115-121. (in Japanese)

JCI-S-003-2007. (2007). "Method of test for bending moment–curvature curve of fiber reinforced cementitious composites." Japan Concrete Institute Standard, 7.

Kanakubo, T. (2006). "Tensile characteristics evaluation method for DFRCC." *Journal of Advanced Concrete Technology*, 4(1), 3-17.

Kanda, T., Kanakubo, T., Nagai, S. and Maruta, M. (2006). "Technical consideration in producing ECC pre-cast structural element." *Proceedings of Int'l RILEM workshop on HPFRCC in structural applications*, Published by RILEM SARL, 229-242.

Kanda, T. and Li, V. C. (1999). "Effect of apparent fiber strength and fiber-matrix interface on crack bridging in cement composites." *ASCE J. of Engineering Mechanics*, 125(3), 290-299.

Lepech, M. D. (2006). "A paradigm for integrated structures and materials design for sustainable transportation infrastructure." Ph.D. Thesis, Univ. of Michigan, Ann Arbor.

Li, V. C. (2004). "Strategies for high performance fiber reinforced cementitious composites development." *Proceedings of International Workshop on Advances in Fiber Reinforced Concrete*, Bergamo, Italy, 93-98.

Maalej, M. and Li, V. C. (1994). "Flexural/tensile strength ratio in engineered cementitious composites." *ASCE Journal of Materials in Civil Engineering*, 6(4), 513-528.

Naaman, A. E. and Reinhardt, H. W. (1996). "Characterization of high performance fiber reinforced cement composites (HPFRCC)." in *High Performance Fiber Reinforced Cementitious Composites*, RILEM Proceedings 31, Eds. A. E. Naaman and H. W. Reinhardt, 1-23.

Ostergaard, L., Walter, R. and Olesen, J. F. (2005). "Method for determination of tensile properties of engineered cementitious composites (ECC)." *Proceedings of ConMat'05*, Vancouver, Canada.

Qian, S. and Li, V. C. (2007). "Simplified inverse method for determining the tensile strain capacity of SHCCs." *Journal of Advanced Concrete Technology*, 5(2), 235-246, June 2007.

Stang, H. and Li, V. C. (2004). "Classification of fiber reinforced cementitious materials for structural applications." *Proceedings of BEFIB*, Varenna, Lake Como, Italy, 197-218.